Journal of Energy Storage 51 (2022) 104596

Contents lists available at ScienceDirect

Journal of Energy Storage

journal homepage: www.elsevier.com/locate/est

Research Papers

IoT real time system for monitoring lithium-ion battery long-term operation in microgrids

Isaías González *, Antonio José Calderón, Francisco Javier Folgado

Department of Electrical Engineering, Electronics and Automation, Universidad de Extremadura, Avenida de Elvas, s/n, Badajoz 06006, Spain

ARTICLE INFO

Keywords:
Lithium-ion battery
Microgrid
Photovoltaic
Monitoring
Internet of things
Grafana

ABSTRACT

Energy storage through Lithium-ion Batteries (LiBs) is acquiring growing presence both in commercially available equipment and research activities. Smart power grids, e.g. smart grids and microgrids, also take advantage of LiBs to deal with the intermittency of renewable energy sources and to provide stable voltage. In this context, monitoring and data acquisition tasks are required for the proper operation and continuous surveillance and tracking of the LiB. In this paper, a monitoring system devoted to visualizing the operation of a LiB is presented. Internet of Things (IoT) technology is used to deploy the system, namely, Grafana software is applied for data analytics and visualization, being hosted in a microcomputer Raspberry Pi. The user is able to access online to graphical and numerical real time information about the LiB magnitudes (current, voltage, temperature, state of charge, etc.). Such a LiB acts as the backbone of a microgrid which hybridizes photovoltaic power with hydrogen generation and consumption. The proposal is a novelty in scientific literature since it overcomes limitations identified in previous works such as absence of long-term operation, of medium-scale power/capacity, of alerts for safe range of critical magnitudes, of real operating conditions, and of compatibility/interoperability management. The design and implementation of the monitoring system is reported together with experimental data of the LiB to prove its feasibility and successful performance.

1. Introduction

Energy storage by means of Lithium-ion Batteries (LiBs) is achieving greater presence in the market as well as important research and development (R&D) efforts due to its advantages in comparison with other battery technologies. Among these advantages, long life cycle, high power density and low self-discharge rate are found [1,2]. These batteries are equipped with Battery Management Unit (BMU), also called Battery Management System (BMS), built by the manufacturer and devoted to measuring magnitudes like voltage, current and temperature, cell balancing, as well as to control the charge/discharge cycles under safe conditions. The BMU is provided by the manufacturer so its operation and configuration is transparent for the user, who can only access to certain magnitudes like current, voltage, temperature and State of Charge (SOC). Nonetheless, there is also ongoing research works about BMU [3] design.

Concerning energy facilities, battery-based storage systems are considered as an essential building block for a transition towards more sustainable and intelligent power systems [4]. For microgrid scenarios, batteries provide short-term energy accumulation and act as common DC voltage bus where consumption and generation equipment are connected. This way, intermittent variations of renewable power sources are smoothed by the batteries, providing a stable voltage and power flow to the loads [5]. This function is even more relevant in isolated or off-grid microgrids, which operate in an autonomous manner. In particular, LiBs have been reported as energy storage system for microgrids in recent works. In [6] the management of a microgrid combining photovoltaic (PV) generation, electric vehicles and a LiB is studied, whereas in [7] such a LiB is modeled from experimental data. In [8], a LiB is the DC bus of a PV-hydrogen microgrid where a communication multi-layered architecture is developed and applied. Operation strategies for power converters in microgrids that combine renewable sources and LiBs are analyzed in [9]. According to [10], Lithium-ion technology could quickly dominate isolated microgrid applications and contribute to their sustainability.

On the other hand, supervisory and monitoring systems are becoming an essential part of electric power systems [11], and their relevance for energy-related platforms has been highlighted in recent

* Corresponding author.
E-mail addresses: igonzp@unex.es (I. González), ajcalde@unex.es (A.J. Calderón), ffolgar@unex.es (F.J. Folgado).

https://doi.org/10.1016/j.est.2022.104596
Received 22 January 2022; Received in revised form 8 March 2022; Accepted 2 April 2022
Available online 6 April 2022

works. For example, for wind turbines, data from monitoring and supervisory systems are applied for real time operation as well as diagnostics [12]. To monitor PV facilities, a number of developments to collect and display the main variables (power, current, irradiance, etc.) are reported in literature [13–15]. For smart grids and microgrids, the monitoring task is of paramount importance [11,14]. Supervisory systems are considered an essential infrastructure to evolve towards an energetic framework featured by decentralized generation [16]. One of the success factors of microgrids deployment refers to operator training and user-friendly interfaces to easily and consistently maintain the microgrid normal operation [17]. Different visualization methods used in smart grids are reviewed and evaluated in [18], which highlights the key role of visualization in facilitating monitoring and analysis in smart power grids.

Nowadays, a prominent trend in the deployment of monitoring systems relies on using Internet of Things (IoT) hardware and software. Integrating IoT environment in energy systems aids for remote monitoring and for efficient energy management [19]. As signaled in [20], recent literature about IoT open-source applications shows versatility, applicability, usability, affordability, and available support, among other advantages. To support microgrid applications, the IoT technology provides great opportunities for sensing, communication, processing, and actuating [21].

Despite the abovementioned importance of monitoring systems, there is very scarce literature about these systems applied to batteries and, in particular, to LiBs. Hereafter, the most relevant contributions in this regard are commented. Certain works that design BMUs are included due to the similarities of equipment (software and hardware) that are used. In [22] a programmable logic controller is used to implement a BMU for LiBs while a Human-Machine-Interface allows to visualize the magnitudes. A small-scale battery (3.2 Ah) is used as experimental case. Thomas et al. [23] design a BMU for LiBs using a microcontroller which provides a HyperText Markup Language (HTML) web interface to visualize electrical variables (voltage and current). Such web page is hosted on an external server, namely Hostinger. An open-source BMU is designed in [24], using the microcontroller Arduino and Node-RED for data acquisition and visual display, respectively. Lezynski et al. [25] present a controllable cyber-physical system to characterize different types of batteries, using LabVIEW to configure the tests and display experimental data. However, such a system is solely focused on testing batteries, not on continuous monitoring of their magnitudes and operation. Some papers briefly mention the software/hardware equipment used to characterize LiBs for example for SOC estimation. For instance, LabVIEW is applied in [26,27].

The development of a low-cost supervisory system for microgrid testbeds is presented in [11]. An HTML user interface, hosted on a Plesk server, provides data about the microgrid components, which are collected by a Raspberry Pi and Arduino boards. A Lead-Acid Battery (LAB) is included in the microgrid but there is no data reported about its operation. A monitoring system for microgrid including a Vanadium Redox Flow Battery (VRFB) is designed in [28]. The proposal combines a Raspberry Pi with commercial energy meters, and web platform ThingSpeak to display data. Hosseinzadeh et al. [29] develop a monitoring platform for distributed energy resources, including a LAB. LabVIEW is used for local monitoring and Grafana for web-enabled visualization. An exception is found in [6], where a LiB of 5.0 kW is used in the context of a microgrid. In that proposal, instead of using a monitoring system, data from the battery is collected by means of a JavaScript Object Notation (JSON) library instead of using real time data.

Additionally, there are valuable papers which assert that a monitoring system has been deployed, but there is no information about its design (software, communications, etc.) and/or it is not shown including measured data. Recent examples can be found in [30–32].

Therefore, according the performed literature review, to date there are no previous works about monitoring systems using IoT technology applied to LiBs.

Moreover, in many cases, there are scarce details about relevant aspects such as communication linkages and/or data treatment, this information being helpful to spread LiB-based facilities. In this regard, given the growing availability of LiBs in the market, it is necessary to provide information about interoperability and compatibility between commercial devices and research-oriented equipment. This type of activities imposes requirements like flexibility, high configurability, scalability and deep control of data treatment given the amount of modifications, analyses and experimental tests to be carried out [33,34].

Most of surveyed papers report data of LiB operation during short-term periods. For instance, the works in [35,36] report data for six days; in [28] data from four days are shown; reference [25] provides data from experiments lasting around 200 s; less than two hours are reported in [22]. In [37], data from 6 months of continuous operation of LABs in the context of a PV-wind hybrid system are reported. However, information about the monitoring system is not provided in this last publication. The power/capacity of the studied LiB is also variable in previous works given the fact that small-scale LiBs are managed in [22,23], whilst medium-scale batteries are used in [6,8,23,35,36]. In a similar sense, real operating conditions of LiBs are not commonly reported since many works refer to laboratory conditions [22,23,25], which could not be representative of medium or long-term operation of the LiB. On the contrary, the works in [8,11,35,36] provide information of real-world operation.

The majority of reviewed papers about monitoring systems include only certain magnitudes of the battery, for example voltage and current, omitting essential values like its SOC and temperature. The SOC is the most illustrative magnitude of the battery state; it represents the available remaining capacity and is a non-measurable internal state [38]. Regarding battery temperature, it is one of the most crucial parameters for safe and reliable operation of Li-ion cells [39]. Indeed, thermal instability and temperature-dependent nonlinear behavior are among the common concerns behind the safe and reliable operation of LiBs [40]. Consequently, LiB temperature must be continuously monitored not only by the BMU but also by the user of the battery, and, even more, this magnitude must be recorded for analytics.

Another lack that has been detected is referred to the absence of alerts generation concerning magnitudes of the LiB. Alerts are of great importance in monitoring tasks for microgrids [41], even more when managing complex and sophisticated equipment. However, in the reviewed literature concerning LiB monitoring, none of the previous works report the generation and/or utilization of alerts to ensure the correct ranges of the battery magnitudes.

Moreover, the general approach consists on representing the LiB variables evolution combined with signals from other components. This is useful for visualization of the whole operation but, in a certain sense, reduces the relevance of the LiB and makes more difficult the proper tracking and surveillance of its operation. Therefore, such relevance of the energy storage device in the power microgrid deserves the development of a monitoring system specifically devoted to acquiring, recording, analyzing and displaying in real time the LiB magnitudes and operation.

On the view of the surveyed literature, there are several research gaps that need to be fulfilled. Namely, long-term data, medium-scale LiB, and alerts to track safe range values of critical magnitudes such as SOC and temperature have to be included in LiB monitoring systems. In addition, performance under real operating conditions as well as guidelines to solve compatibility and interoperability issues are also added values.

With the goal of overcoming the aforementioned research gaps, this paper presents the design of a monitoring system based on IoT technology for a LiB integrated in a Battery-powered Hydrogen Microgrid (BHMG). The LiB is a Lithium iron phosphate battery of 5.0 kW manufactured by BYD. The data provided by the in-built BMU is transmitted to an in-house IoT server and displayed through a user interface developed

using the software Grafana. Online access to real time information on LiB magnitudes is achieved. According to the conducted literature review, this proposal constitutes a novelty in literature.

Previous research works validate the utilization of Grafana for monitoring purposes. In [14], Grafana is applied to track the temperature of a PV array integrated in a microgrid. In [35,36] this software is used for visualizing the operation of a PV array and a LiB for water pumping purposes. For indoor environmental monitoring, Grafana is applied in [42]. Under the IoT framework, a PV plant is monitored by means of Grafana in [15]. Energy monitoring of an industrial asset is developed with Grafana in [43]. This software is also used for data query and visualization in the context of Industrial IoT, as reported in [44].

For a clear comparative presentation of previous publications and the present proposal, Table 1 summarizes the main features classified in the following categories. The category Software (SW) corresponds to the software environment to display and visualize data. Hardware (HW) refers to the device where the software runs. Communication is the linkage used to gather the data to be displayed. Long-term data applies for time intervals longer than one month. IoT is marked as affirmative if there is IoT hardware or software. Battery (type; rated power or capacity) indicates whether a battery is included in the monitored devices and, in affirmative case, its type and power or capacity. Alerts, temperature and SOC indicate whether the work reports alert generation, battery temperature and SOC, respectively.

The development presented in this paper is framed within a R&D project to develop digital twins of BHMGs. The aim of this work is twofold. On the one hand, massive data acquisition for digital replication of the LiB is required. On the other hand, overcoming the limitations of data storage provided by the manufacturer of a gateway compatible with the LiB is a necessity. For both motivations, IoT technologies bring solutions capable of acquiring, transmitting, storing and displaying the magnitudes of a LiB.

The most relevant contributions of the present proposal are listed for sake of clarity:

- IoT technology (hardware and software) is applied to monitor the LiB providing real time data display and accumulation.
- Remote web-based visualization of battery magnitudes and parameters in the form of dynamically updated time-series.
- Automatic surveillance of LiB temperature and SOC is achieved through alerts to inform the operator of dangerous situations.
- Long-term data (two years) of continuous operation of both the LiB and the monitoring system are reported.
- Medium-scale (5.0 kW) LiB is monitored under real operating conditions.
- Compatibility/interoperability is successfully handled by means of IoT protocol widely supported by power equipment.
- Novelty in literature, overcoming drawbacks identified in previous works.

The structure of the rest of the article is as follows. The materials and methods used in the research are described in the second section. The third section reports the design of the monitoring system. Experimental results are expounded and discussed in the fourth chapter. Finally, the main conclusions of the work are found.

2. Materials and methods

In this section, the monitored LiB, the microgrid where it is integrated, and hardware and software components are described.

2.1. Lithium-ion battery

The use of Lithium technology is a modern trend in battery manufacturing. LiBs are being investigated from a number of perspectives, from their utilization in electric vehicles [45] to improvements of cells and cathodes materials. Other activities deal with remaining energy prediction [46], remaining useful lifetime prediction [47,48], temperature estimation [40,49], SOC and State of Health (SOH) estimation [38,50–57], study of degradation and aging mechanisms [58], modeling based on equivalent circuit models (ECM) [59] or on data-driven methods [1], and developments about instrumentation and sensing technologies [60]. An in-depth review about research on LiBs can be found in [39].

In the present work, a $LiFePO_4$ battery model B-Box Pro 5.0, manufactured by BYD, is the monitored LiB. It acts as the backbone of a BHMG where PV power is used to produce hydrogen by means of water electrolysis. Energy flows take place around the LiB; hence, it materializes the low voltage DC bus of the microgrid. This battery is composed of two modules U3A1-50P-A [61] connected in parallel providing a maximum power of 5.0 kW at a nominal voltage of 51.2 V. Concerning communication capabilities, the modules are connected among them and with the BMU via Controller Area Network (CAN) bus over RS485 interface. The main technical characteristics of the LiB are seen in Table 2.

The chemical reactions that take place in $LiFePO_4$ batteries are as follows. During discharge process, lithium ions detach from the graphite

Table 1
Comparison of main features of previous works and present proposal.

Work	SW	HW	Communication	Long-term data	IoT	Battery (type; power/capacity)	Alerts	Temperature	SOC
[11]	HTML	Plesk server	TCP/IP	No	Yes	Yes (LAB; 12 kWh)	No	No	No
[43]	Grafana	Raspberry Pi	Modbus RTU	No	Yes	No	No	No	No
[15]	Grafana	Raspberry Pi	MQTT	No	Yes	No	No	No	No
[23]	HTML	External hosting	WiFi	No	No	Yes (LiB; 10 Ah)	No	Yes	No
[24]	Node-RED	IBM server	MQTT	No	Yes	Yes (LiB; 2.5 Ah)	No	No	Yes
[35,36]	Grafana	Raspberry Pi	Gateway + Modbus TCP/IP	No	Yes	Yes (LiB; 3.3 kW)	No	No	Yes
[25]	LabVIEW	PC	Gateway + Modbus TCP/IP	No	No	Yes (various types; 100 Ah)	No	No	No
[28]	ThingSpeak	Raspberry Pi	Modbus TCP/IP	No	Yes	Yes (VRFB; 1 kW)	No	No	No
[22]	WinCC	PC	TCP/IP	No	No	Yes (LiB; 3.2 Ah)	No	No	Yes
[29]	LabVIEW + Grafana	PC	Modbus TCP/IP	No	No	Yes (LAB; 200 Ah)	No	No	No
[8]	Grafana	Raspberry Pi	Gateway + Modbus TCP/IP	No	Yes	Yes (LiB; 5.0 kW/100 Ah)	No	No	Yes
[14]	Grafana	Raspberry Pi	Gateway + Modbus TCP/IP	Yes	Yes	No	Yes	No	No
Present work	Grafana	Raspberry Pi	Gateway + Modbus TCP/IP	Yes	Yes	Yes (LiB; 5.0 kW/100 Ah)	Yes	Yes	Yes

Table 2
Main characteristics of the LiB B-Box Pro 5.0.

Characteristic	Value
Battery type	$LiFePO_4$
Number of U3A1-50P-A modules	2
Nominal voltage	51.2 V
Voltage range	43.2–56.4 V
Max output power	5.0 kW
Nominal capacity	100 Ah
Ambient temperature range	−10 + 50 °C
Operating temperature	Charge: −10 + 50 °C Discharge: −20 + 55 °C
Enclosure Protection	IP20
Communication	CAN – RS485

of the anode and travel to the cathode through the electrolyte. Electrons are also released from the anode and provide electric current out of the battery. In the charging process, lithium ions and electrons are separated from the iron phosphate of the cathode and transferred to the anode. The overall electrochemical reaction is seen in Eq. (1) [59]:

$$Li_nC_6 + Li_{m-n}FePO_4 = Li_0C_6 + Li_mFePO_4 \quad (1)$$

As indicated in the previous section, the SOC is a paramount magnitude of LiBs. It is commonly applied as a control parameter in battery-based infrastructures like microgrids [6,62,63], being used in the Energy Management Strategy (EMS) to determine operation thresholds and logical decisions to manage power flows and interactions between generators, loads and batteries taking into account data from a multiplicity of sensors. The SOC can be expressed as a percentage and illustrated through Eq. (2):

$$SOC = (Qr/Q_N)*100\% \quad (2)$$

where Qr stands for the remaining capacity and Q_N is the rated capacity under the same conditions. However, Qr is difficult to be determined in a direct manner, so the most commonly used method for SOC calculation corresponds to the ampere-hour integral formula, Eq. (3) [64]:

$$SOC = SOC_0 + \frac{1}{Q_N}\int_0^t \eta I dt \quad (3)$$

where the initial SOC is SOC_0, η is the performance of the charging/discharging processes, and I is the battery current. This method is easy to implement and requires low computational resources. However, the main disadvantage of this method is the large cumulative error for long-term. Moreover, there are a number of different estimation techniques in literature such as Kalman Filter [56,57,64–66], fuzzy logic-based approaches [67], neural networks [68] or least squares-based methods [51–53], which proves the relevance of this parameter to properly monitor and manage LiBs.

Overcharging and over-discharging can cause permanent damage to the LiB [69], so the SOC must be kept within a safe range according to Eq. (4):

$$SOC_{min} < SOC < SOC_{max} \quad (4)$$

where both extreme values must be adjusted taking into consideration the manufacturer data as well as operational boundaries established by the EMS, being exemplary values 20% and 95%, respectively.

2.2. Battery-powered hydrogen microgrid

The LiB acts as short-term energy storage medium of a microgrid devoted to producing green hydrogen from PV generation. To this aim, distributed generation and consumption of both electricity and hydrogen take place around the LiB. A PV array composed of 6 monocrystalline modules is responsible for converting the incident solar irradiance into electricity to feed the LiB and an electronic programmable load. A Hydrogen-fueled Polymer Electrolyte Fuel Cell (HPEFC) plays the role of a power generation unit that converts hydrogen into electricity. The required hydrogen is produced through water electrolysis by a low pressure Polymer Electrolyte Water Electrolyzer (PEWE). Hydrogen is stored by means of a Metal-Hydride Tank (MHT), acting as hydrogen buffer to support the input and output flows. For the electrical connection of these components to the LiB, DC-DC power converters are needed. A buck converter links the PEWE to the DC bus, and the HPEFC requires a boost converter. Finally, a solar charger with Maximum Power Point Tracking (MPPT) connects the PV array to the LiB. Fig. 1 depicts the diagram and interconnections of the microgrid, and Table 3 contains the most relevant characteristics of the described components.

The microgrid operates in an autonomous off-grid mode by performing a power balance to determine the energy dispatch between generation and consumption components. In particular, Eq. (5) illustrates the power balance, where P corresponds to the power provided or consumed by each component:

$$P_{PV} + P_{HPEFC} + P_{LiB} + P_L + P_{PEWE} = 0 \quad (5)$$

Fig. 2 depicts the flowchart of the power dispatching algorithm. The load and the LiB are supplied by the PV array and the LiB SOC is evaluated. If this parameter is above the threshold SOC_{max} and there is available PV power, the hydrogen production takes place by means of the PEWE. If the battery is discharged, i.e. the SOC is below SOC_{min} and there is available hydrogen, the HPEFC is switched on to generate power and feed the load. This way, the generation of hydrogen from PV source and its consumption enables an autonomous and environmental-friendly behavior.

Additional components required for the operation of the LiB-based microgrid are now briefly expounded. To begin with, GX is a gateway and controller for power devices such as inverters, solar chargers or BMUs. It is manufactured by Victron Energy and enables data exchange by means of IoT communication protocols. Raspberry Pi is an inexpensive single-board microcomputer that provides high computational resources as well as support for a number of communication protocols. It runs operative system based on Linux and is widely used in the IoT framework. The version 4 model B has been applied in the present work. Concerning software, three main packages are used, all of them of open-source type and widely used in IoT frameworks. To begin with, Grafana is an environment to build time-series graphs and general purpose dashboards. It is a web-based tool that allows data query, analytics and visualization [44]. MariaDB is a relational database that uses Structured Query Language (SQL) for data access, is derived from MySQL and is fully compatible with Grafana. Finally, PHPMyAdmin is a database management system oriented to facilitate the administration of MySQL and mariaDB operations. It runs on a web environment and is written in PHP.

3. Developed IoT Monitoring system

The presented monitoring system allows for continuous recording and display of LiB magnitudes. These data are collected from equipment to which the LiB is directly connected. Namely, the BMU of the LiB measures the voltage, current and temperature, and estimates the SOC. The GX gateway retrieves this information and makes it available for other equipment. On the other hand, the MPPT solar charger, from Victron Energy manufacturer, is also integrated to manage the PV production. This device is connected to the gateway through a proprietary bus, VE.Direct, so its measurements are also available for monitoring tasks. Table 4 summarizes the signals that are provided by the BMU and the MPPT (data sources), accessible by the gateway, and retrieved and shown by the developed monitoring system.

Compatibility and interoperability issues arise when heterogeneous equipment (hardware and software) are integrated. Systems integration is a vital task for seamless data exchange and communication that

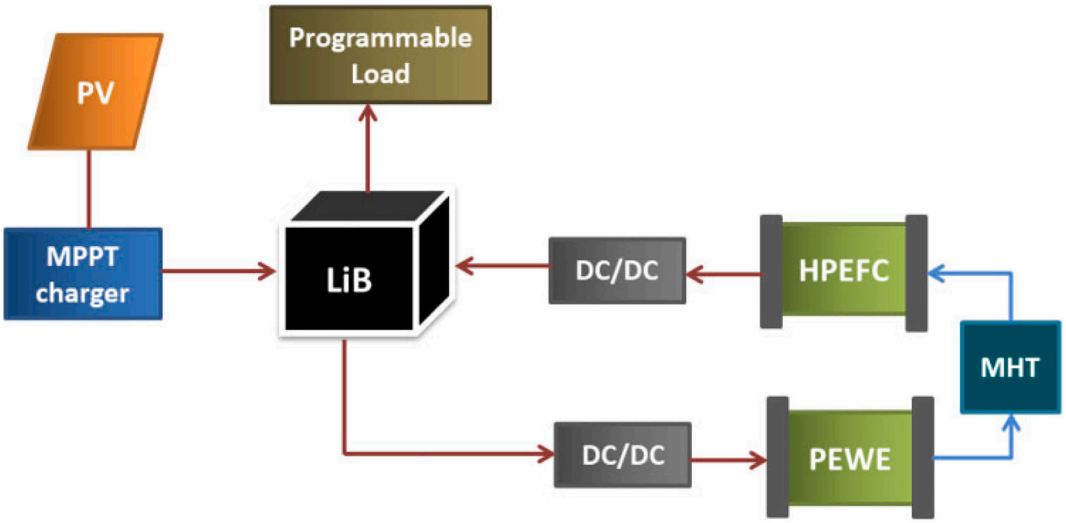

Fig. 1. Diagram of the LiB-supported microgrid.

Table 3
Main characteristics of the microgrid equipment.

Equipment	Characteristics
PV array	6 modules, monocrystalline technology, 1.1 kW
PEWE	18 cells, 750 mLN/min
HPEFC	32 cells, 0.5 kW
Load	AC/DC programmable, 5.4 kW
H_2 buffer	Metal-hydride tank

requires severe efforts [70]. A variety of communication protocols are available and must be selected in a proper manner. Standardized interfaces and protocols must be used to handle compatibility between nodes [70,71].

Concerning LiBs, the connectivity options of the corresponding BMU determines the available communication protocols and must be taken into account during the design and deployment of the facility to properly share information. The GX gateway provides two open communication protocols for sharing data, Message Queuing Telemetry Transport (MQTT) and Modbus TCP/IP. Modbus was developed in 1979 by

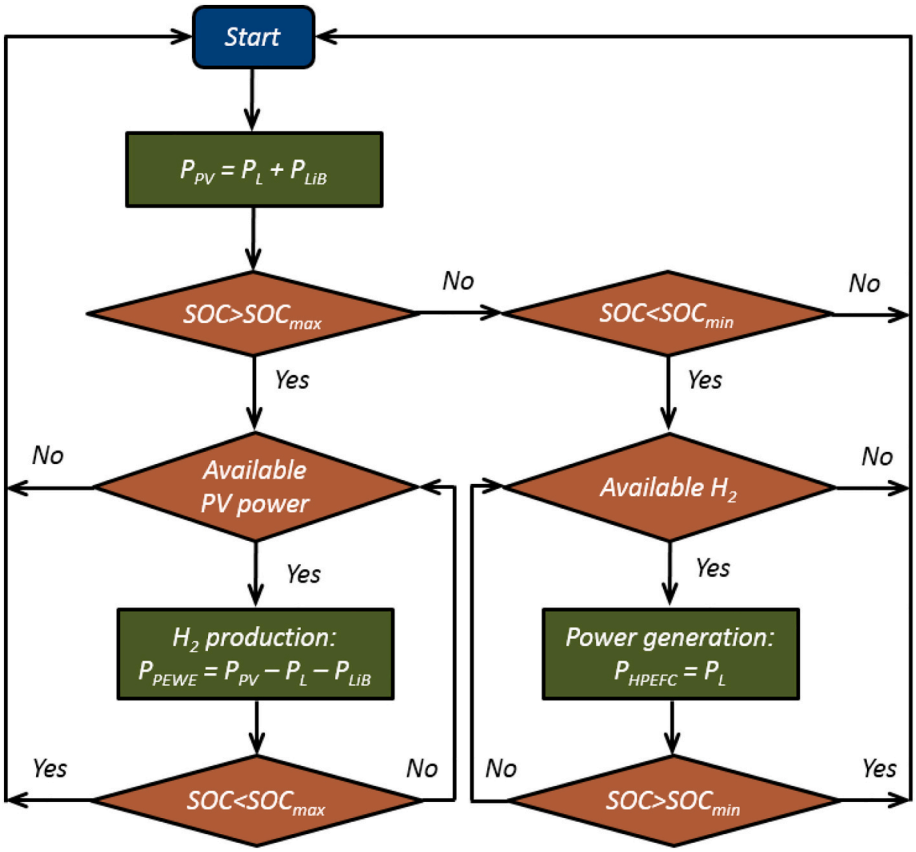

Fig. 2. Flowchart of the power dispatching algorithm.

Table 4
Magnitudes and data source device.

Magnitude	Data source
LiB current	BMU
LiB voltage	
LiB SOC	
LiB temperature	
LiB power	
PV current	MPPT
PV voltage	
PV power	

Modicon (currently Schneider Electric) for data transmission in industrial automation assets and its simplicity and open nature led it to become a de facto standard [8]. The latest version of this protocol is the Transmission Control Protocol/Internet Protocol (TCP/IP) with client/server architecture over Ethernet networks. In fact, this TCP/IP version is signaled as IoT communication protocol in [72] and is widely supported by power-related equipment [8].

For these reasons and taking into consideration the aforementioned devices, a communication network based on Ethernet and Modbus has been designed to integrate them and allow online monitoring of the LiB information. The GX acts as Modbus server, making accessible the data gathered from the BMU and the solar charger. On the opposite, a Python script acts as middleware responsible for acquiring data from the gateway memory, in other words, it plays the role of Modbus client. This way, LiB operational information is acquired by the middleware and stored in a database implemented with mariaDB. Both the middleware and the database run on a Raspberry Pi. The same device acts as server for the software Grafana so remote online access through the Internet is enabled. The developed monitoring system and the corresponding communication network are depicted in the diagram shown in Fig. 3.

As aforesaid, data accumulation is carried out by means of a mariaDB database that records the LiB-related magnitudes with a sampling time of 1 min. PHPMyAdmin is used to manage this database through a web browser, as can be seen in Fig. 4, where the battery voltage, current, temperature and SOC are stored.

With respect to data visualization, a Grafana dashboard containing graphical charts and instant numeric values is accessed online by the user. The data is queried from databases and displayed through common web browsers. Hence, the remote user does not require installing packages on the device. The user must access to the IP address and logical port of the IoT server by means of a web browser in a computer, mobile phone or tablet. Therefore, data can be displayed locally and over the network [73].

In the present proposal, Grafana runs in the Raspberry Pi, which acts as in-house IoT server accessible from the network. In this regard, a noteworthy remark deals with the utilization of hosting platforms owned by service providers, which is considered as a limitation since it creates dependencies. Hosting through own servers implies a total control of administration aspects and isolation of failure situations (connectivity network or server crashes) [14].

The procedure to visualize LiB data through Grafana requires two interactions (see Fig. 5). On the one hand, the remote user connects to the IoT server via web browser and selects the desired time interval, as well as a specific panel if required. On the other hand, the LiB data is stored and available in the database for queries. Thus, Grafana reads the established data from the database and displays the corresponding time-series graphs, instant values and alerts.

4. Results and discussion

The experimental results obtained of the LiB operation in the microgrid are reported in this section aiming at proving the suitability of the developed monitoring system. Moreover, a discussion of such results and the main findings is carried out in the second subsection.

4.1. Results

4.1.1. Experimental setup

Fig. 6 shows the laboratory experimental setup where the used components are interconnected. To begin with, the LiB is composed of two modules connected in parallel and the BMU placed on the top, being

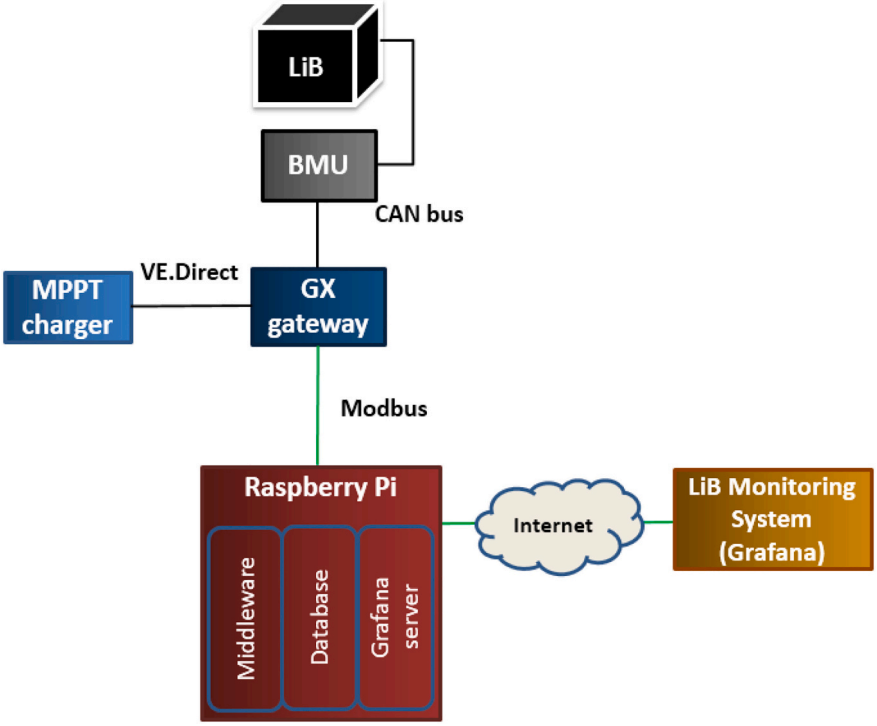

Fig. 3. Diagram of the monitoring system and the communication network.

idgx 1	datetimegx	secondsgx	batvoltagegx	batcurrentgx	battempgx	batstategx
928258	2021-12-09 13:05:02	0.339143	53.90	2.00	19.00	99.00
928257	2021-12-09 13:04:02	0.30235	53.88	2.20	19.00	99.00
928256	2021-12-09 13:03:02	0.275119	53.88	2.20	19.00	99.00
928255	2021-12-09 13:02:02	0.281429	53.85	2.30	19.00	99.00
928254	2021-12-09 13:01:02	0.312552	53.82	2.20	19.00	99.00
928253	2021-12-09 13:00:01	0.391056	53.82	2.30	19.00	99.00
928252	2021-12-09 12:59:01	0.333562	53.79	2.10	19.00	99.00
928251	2021-12-09 12:58:02	0.266371	53.75	1.90	19.00	99.00
928250	2021-12-09 12:57:02	0.268154	53.72	1.10	19.00	99.00
928249	2021-12-09 12:56:02	0.332397	53.70	1.50	19.00	99.00
928248	2021-12-09 12:55:02	0.260324	53.69	1.10	19.00	99.00
928247	2021-12-09 12:54:02	0.30481	53.67	0.60	19.00	99.00
928246	2021-12-09 12:53:01	0.305338	53.67	0.60	19.00	99.00
928245	2021-12-09 12:52:01	0.292304	53.67	0.50	19.00	99.00
928244	2021-12-09 12:51:01	0.290553	53.67	0.50	19.00	99.00

Fig. 4. Aspect of the mariaDB database for LiB monitoring.

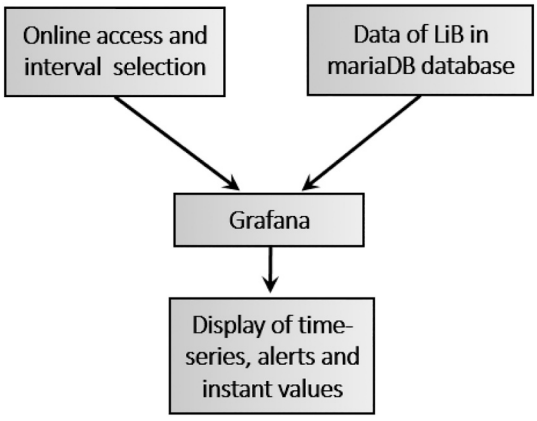

Fig. 5. Diagram of the Grafana interactions.

inside a cabinet (Fig. 6a). Other elements also assembled are the MPPT charger, the Raspberry Pi and the GX gateway, as seen in Fig. 6b.

4.1.2. Monitoring interface description

The dashboard has been organized for a rapid inspection of the LiB magnitudes by means of both numerical and graphical information (Fig. 7). In the upper part, instant values can be read, whilst dynamically updated graphical charts represent the evolution over time of two or three variables. Both predefined and customizable time intervals can be chosen by the user, so instant, short and long-term data can be easily displayed. The ability of selecting different presentation intervals is an advantage for R&D projects, among others in renewable energies and battery energy storage [35]. Besides, each panel can be seen in full screen and zoom can be applied to select detailed visualizations. Options like data exportation are available for each panel, so the user can perform local data download corresponding to the selected time interval.

4.1.2.1. Instant values. Instant values of the most relevant magnitudes can be seen through numerical indicators in the form of gauges (Fig. 8). By means of these indicators, the user can observe at a glance the status of the LiB. The gauges can be divided into two or more zones with different colours for a more intuitive and faster interpretation of the shown value. For example, for SOC value three intervals have been defined: red color for SOC below 30% to warn of excessively low value, green color for 30% $<$ SOC $<$ 90%, and blue for the rest, meaning that the LiB is close to full charge. As shown in the figure, all the variables are within adequate ranges (green color) and the battery is in blue color (95%). Moreover, a list of alert messages is included for easy identification of anomalous situations.

4.1.2.2. SOC and current evolution. The SOC and current evolution during the considered interval can be observed in Fig. 9. The first day is a partly cloudy day, which causes variations in the current received by the LiB. The SOC grows from 48% (at 09:50) to a maximum of 96% (at 17:50), which is maintained for approximately half an hour due to the fact that the current provided by the PV array is enough to meet the load demand but there is no enough irradiance to continue charging the battery.

Night discharging starts at 18:13 (18 October 2021) and is due to the current delivered to the load. Particularly, the LiB has negative current values (−2.80 A) since it is an output current. The SOC decreases from 96% to 62% at 08:55. After sunrise, the solar irradiance grows so the LiB is again charged. In fact, the second day corresponds to a typical sunny day situation, the LiB is charged from the abovementioned 62% SOC up to 100% SOC at 15:22, after which the battery current is zero until the sunset (18:48).

4.1.2.3. Balance of currents. The current delivered by the PV array (green curve) is also plotted in a chart together with the battery (yellow curve) and load (black curve) currents for a clear representation of the balance of currents. Note that the displayed PV current corresponds to the values after the conversion performed by the MPPT charger, I_{PVA}. As the power delivered by the PV array varies, the battery current is

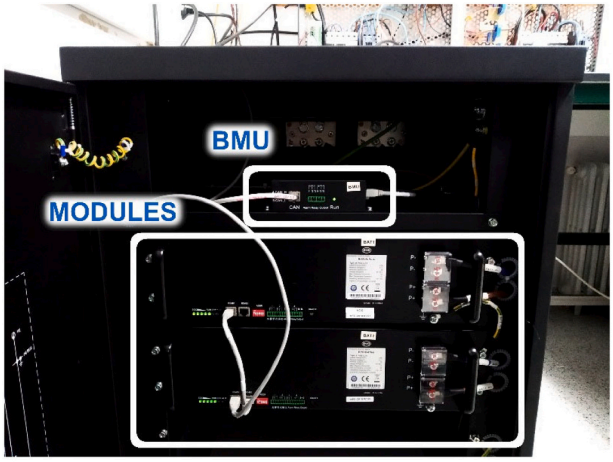

(a)

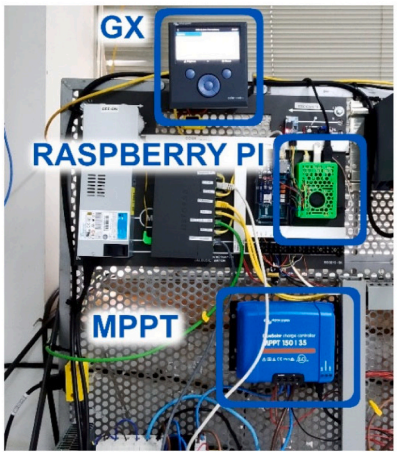

(b)

Fig. 6. Experimental setup: (a) front view of the LiB; (b) Raspberry Pi, GX gateway and MPPT charger.

adapted depending on the demand of the programmable load. Under conditions of irradiance enough to supply the load and charge the LiB, the LiB current represents the current available from solar generation once the load has been satisfied. Thus, the expression for the current LiB is as shown in Eq. (6):

$$I_{LiB} = I_{PVA} - I_L \tag{6}$$

The current consumed by the load is programmed to be constant, as can be observed in the black line of Fig. 10.

4.1.2.4. Power and SOC. Regarding power of the LiB, it is obtained by the Eq. (7), so the sign of the current determines whether it is delivered to supply the load (negative current) or consumed, provided by the PV array (positive current):

$$P_{LiB} = I_{LiB} * V_{LiB} \tag{7}$$

where I_{LiB} corresponds to the current of the battery and V_{LiB} is the LiB voltage, which is coincident with the DC bus voltage. On the other hand, the PV power can be calculated by the Eq. (8):

$$P_{PV} = I_{PVB} * V_{PV} \tag{8}$$

where I_{PVB} is the current produced by the PV modules before the MPPT charger, and their voltage is V_{PV}. Such charger uses a DC-DC converter to extract the maximum power available for the PV modules and adapt the voltage levels. The efficiency of the MPPT charger is supposed to be 100%, i.e. power losses in this device are considered negligible. Therefore, the power before and after the MPPT charger must be equal, according to Eq. (9):

$$I_{PVB} * V_{PV} = I_{PVA} * V_{LiB} \tag{9}$$

A graph chart is devoted to representing the LiB power (mustard color), PV power (dark green color) and the SOC (burgundy color) over time (Fig. 11). This chart is consistent with that devoted to the balance of currents (Fig. 10); the power curves present the same trends.

4.1.2.5. Voltage and current. The LiB voltage and current are displayed together in the graph depicted in Fig. 12. As previously mentioned, 19 October 2021 is a representative sunny day, so the LiB charging process can be appreciated. To begin with, during the bulk phase, the MPPT charger extracts the maximum available power from the PV generator to supply the load and rapidly recharge the LiB. This phase starts at 09:22, when the voltage is 52.58 V (SOC=62% as seen in previous Fig. 11). The maximum current accepted by the battery during this phase is 12 A (at 13:41). As a consequence of the charge increase, the battery voltage progressively grows up to the maximum voltage reached, 56.21 V (at 15:22). In such a moment, the SOC reaches the maximum value, 100%, and the float stage starts, so the float voltage is applied for the battery to be maintained fully charged. Hence, the voltage is stabilized in 54.89 V (current null) until 18:38.

It must be remarked that after reaching the fully charge state, there is a short transient period of two minutes, during which the LiB provides the load current (−2.80 A) because the MPPT charger must adapt the power extracted from the PV array to the new situation. In fact, the charger has to shift the operating point of the PV array away from the MPP. After sunset, the shortage of solar contribution causes the LiB to supply the load. Namely, the discharge current starts at 20:48 with a value of −2.80 A. Regarding the voltage, it must be kept within the range indicated by the manufacturer datasheet [61], namely, above 40 V and below 56.5 V. Therefore, as it has been observed, the LiB operates within the proper range.

4.1.2.6. Temperature and current. As it was commented in the Introduction, the temperature of the LiB is critical aspect that needs to be tracked. In fact, operation of LiBs outside the safe operating temperature directly affects their cycle life, efficiency, reliability and safety [40]. In this regard, the temperature is very stable during the observed period; it varies between 28 °C and 31 °C (Fig. 13). It must be remarked that the temperature signal is an integer number provided by the BMU.

4.1.2.7. Hourly energy. Apart from displaying time-series, Grafana allows for programming mathematical operations using stored data, promoting the design of custom-tailored graphics. Therefore, to analyze the LiB operation, a bar graph has been created for hourly energy visualization. It displays the energy consumed or provided every hour during the current day or over a selected time interval. Fig. 14 shows the aspect of such graph for 18 and 19 October 2021. During night, the energy extracted from the LiB is 146 Wh (with negative values in the image), whereas the maximum energy absorbed by the battery is 627.13 Wh at 13:00 of the second studied day. Besides, as it was stated for Fig. 12, once the SOC is 100%, the LiB current is null and there is no input/output energy. The bars show that this situation lasts for around three hours, from 15:00 to 17:00. As can be appreciated, the trend of energy is consistent with that of current and power magnitudes plotted in previous figures.

4.1.2.8. Long-term operation data. The approach has been functioning from January 2020 to January 2022, two years, as illustrated in Fig. 15a for the temperature and Fig. 15b for the SOC. Due to the research activity applied to the LiB and to the microgrid, there are brief intervals

Fig. 7. Aspect of the Grafana dashboard devoted to monitoring the LiB.

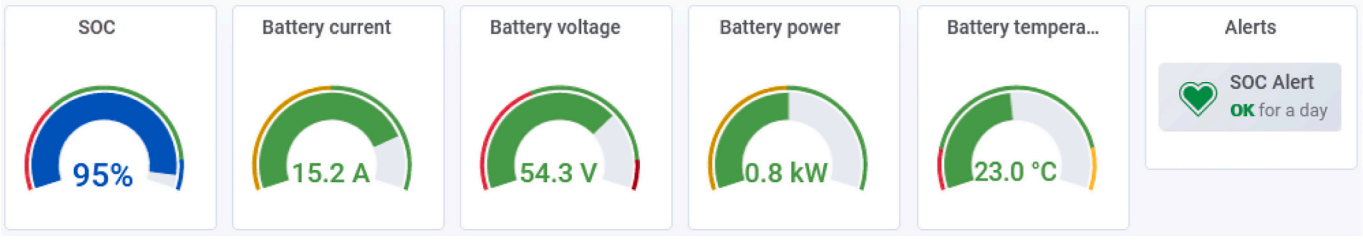

Fig. 8. Detail of instant values indicators in the dashboard.

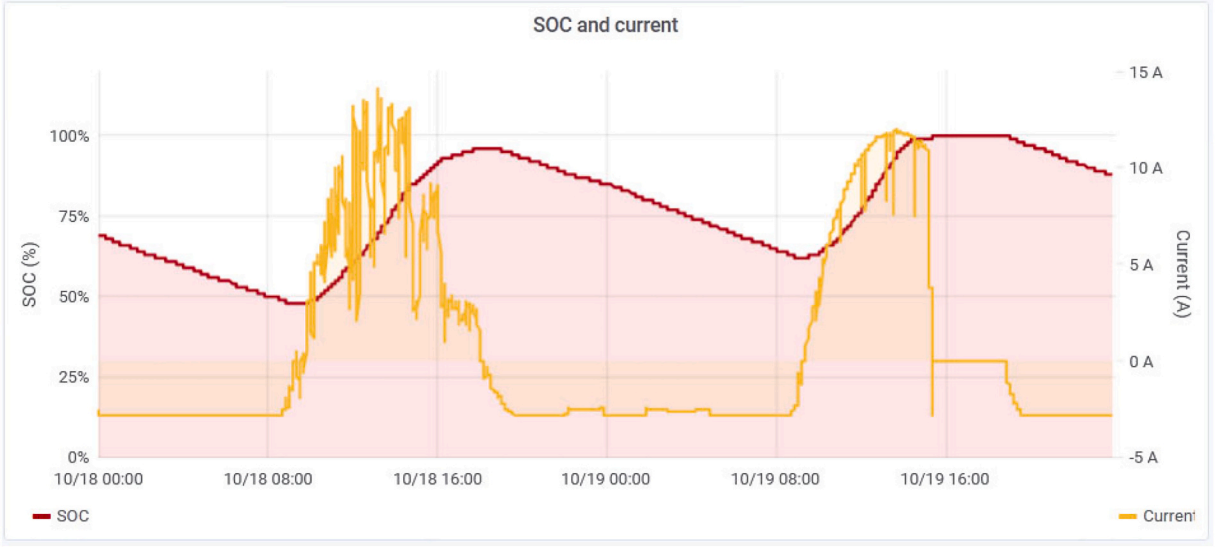

Fig. 9. SOC and current variations during 18 and 19 October 2021.

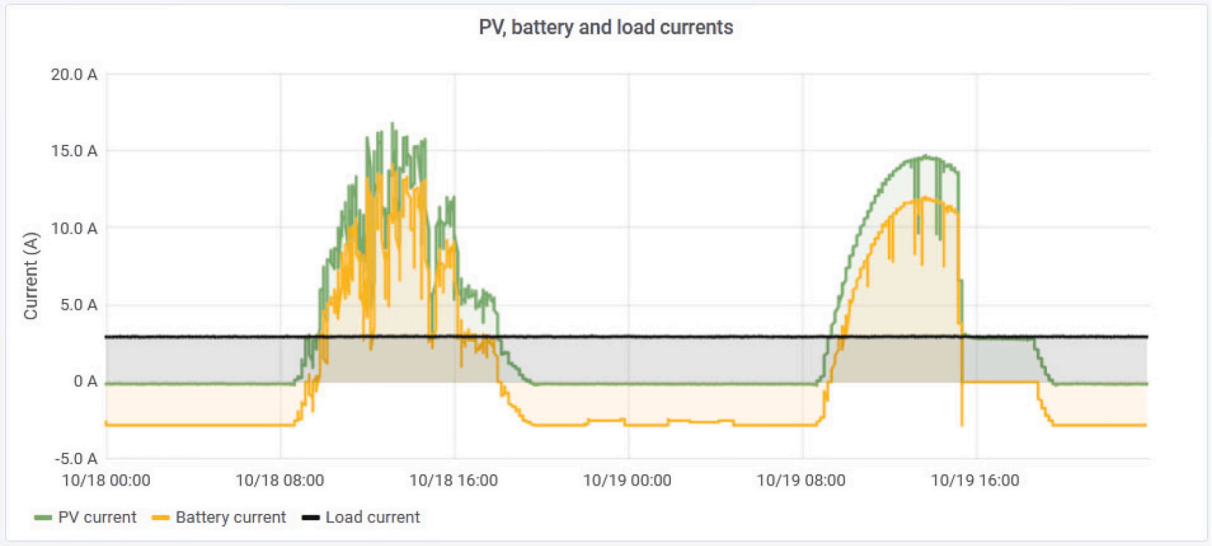

Fig. 10. Balance of currents during 18 and 19 October 2021.

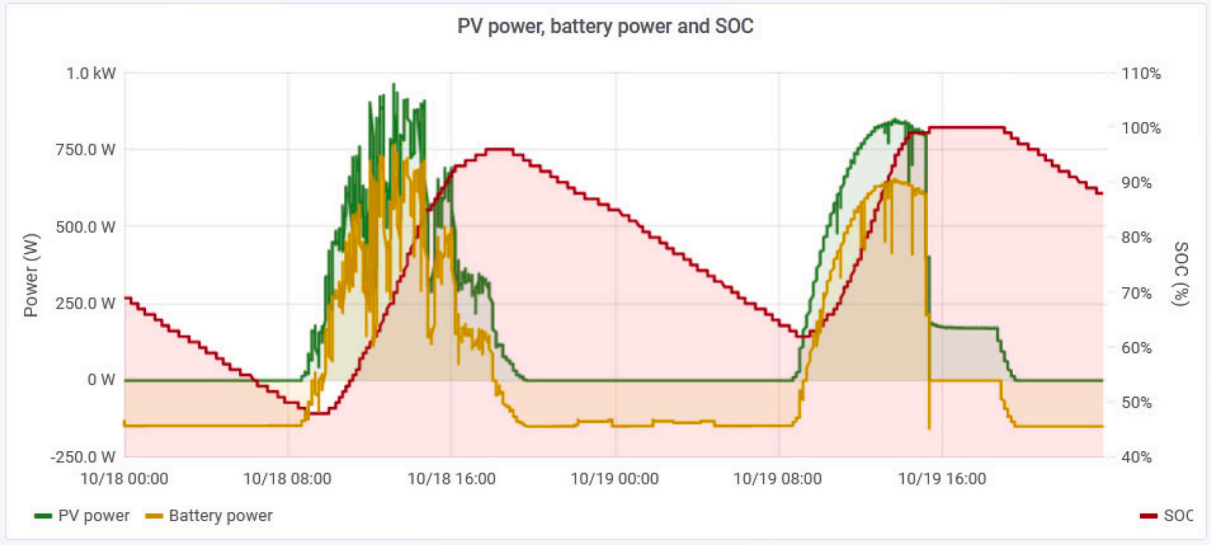

Fig. 11. PV and battery power, and SOC during 18 and 19 October 2021.

without data or with anomalous values. For example, during the initial configuration and establishment of communications, some strange SOC data are found. Concerning temperature, the minimum registered temperature is 13 °C, on 07 January 2021. On the contrary, the maximum temperature that has been reached by the LiB is 38 °C, in August 2021. As can be checked, the measured temperature has always been within the range suggested by the manufacturer (see Table 2).

Concerning the SOC evolution, the minimum SOC (12%) was reached on 21 November 2021. The maximum value, 100 °C, is commonly reached given the great availability of solar irradiance in the zone. Besides, there are various months in which this parameter was continuously kept at 100%, namely, from March to September 2020. During this period, due to the COVID-19 pandemic, the physical access to the laboratory was restricted, so the PV array and the load were disconnected for safety reasons.

4.1.2.9. Alerts generation. Apart from intuitive visualization of the commonly registered variables of LiBs (voltage and current), a set of alerts have been implemented to warn about out of range SOC and temperature values. In this regard, as example, the LiB SOC alert created to prevent from in-depth discharges is expounded. The BMU includes a protection function in this sense, but the user is not able to modify or configure the SOC threshold.

To this aim, the SOC is continuously compared with a reference established by the developer. In this case, a SOC_{min} of 30% has been considered reasonable to limit the degradation of the LiB. If the last sample of SOC during the last five minutes is strictly less than 30%, the alarm is activated. Fig. 16 shows the aspect of the panel devoted to generating and visualizing the alarm. The SOC is plotted over time and the defined threshold is depicted with a horizontal red line. When the SOC value reaches the limit, the alarm is activated and illustrated with a red-colored heart placed on the left of title given to the panel, SOC Alert in this case. Additionally, a vertical dotted line in red color is traced to indicate when the alert is activated. As can be observed in the figure, such a situation took place in 21 November 2021 at 4:11, and the SOC still decreased up to 12% at 9:10, after which PV started to charge the LiB. Once the SOC returns to values within the safe range (at 13:08 in Fig. 16), the heart recovers green color and a vertical dotted line

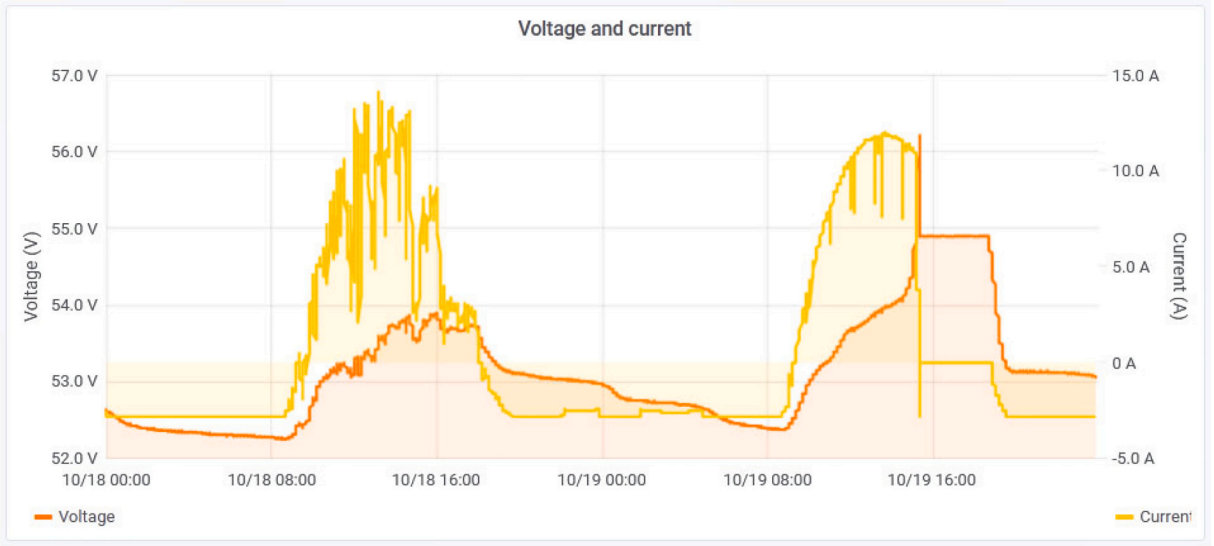

Fig. 12. Voltage and current during 18 and 19 October 2021.

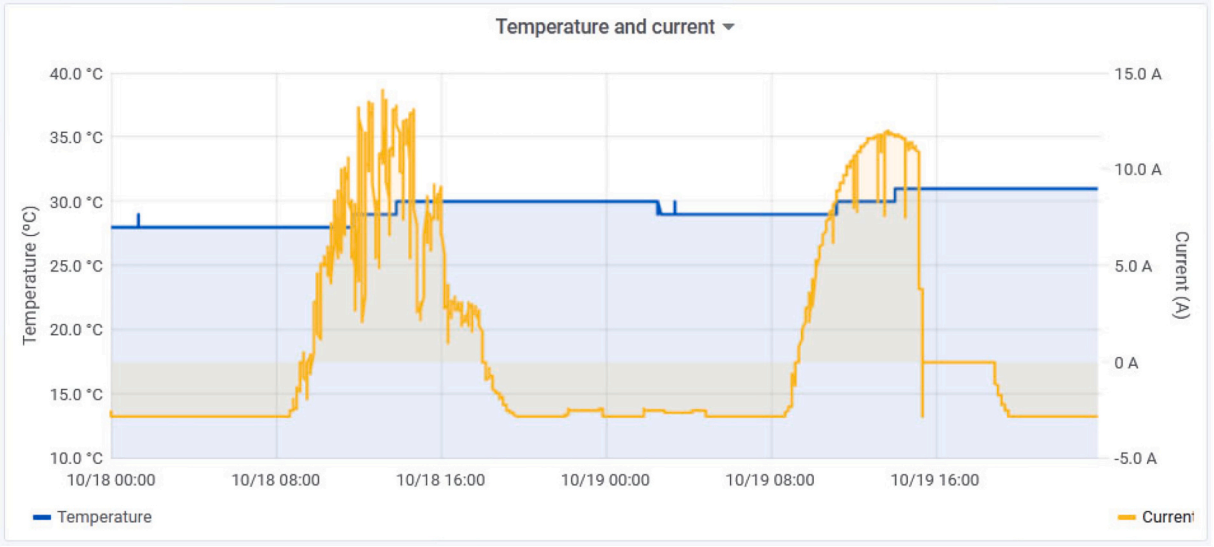

Fig. 13. Temperature and current visualization during 18 and 19 October 2021.

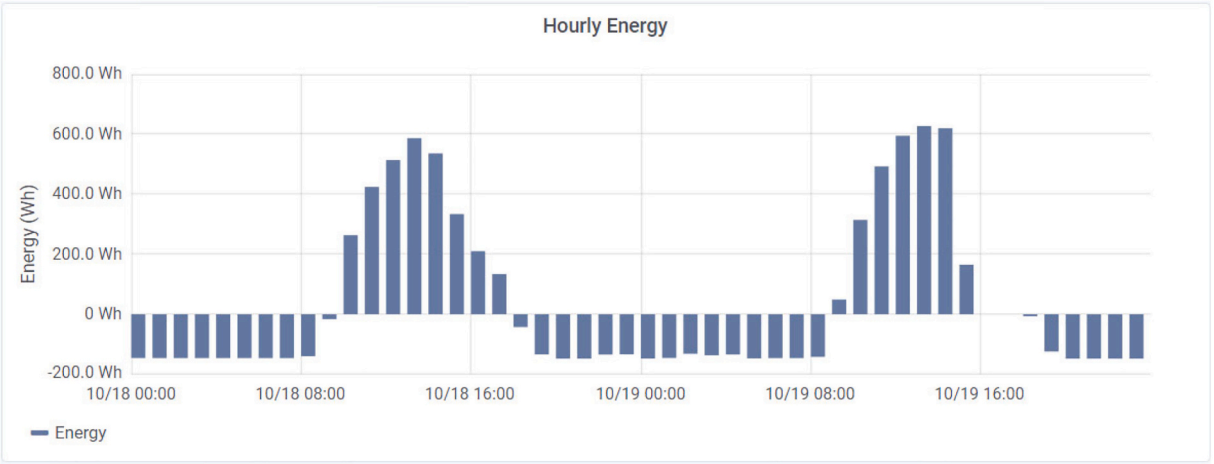

Fig. 14. Hourly energy balance visualization during 18 and 19 October 2021.

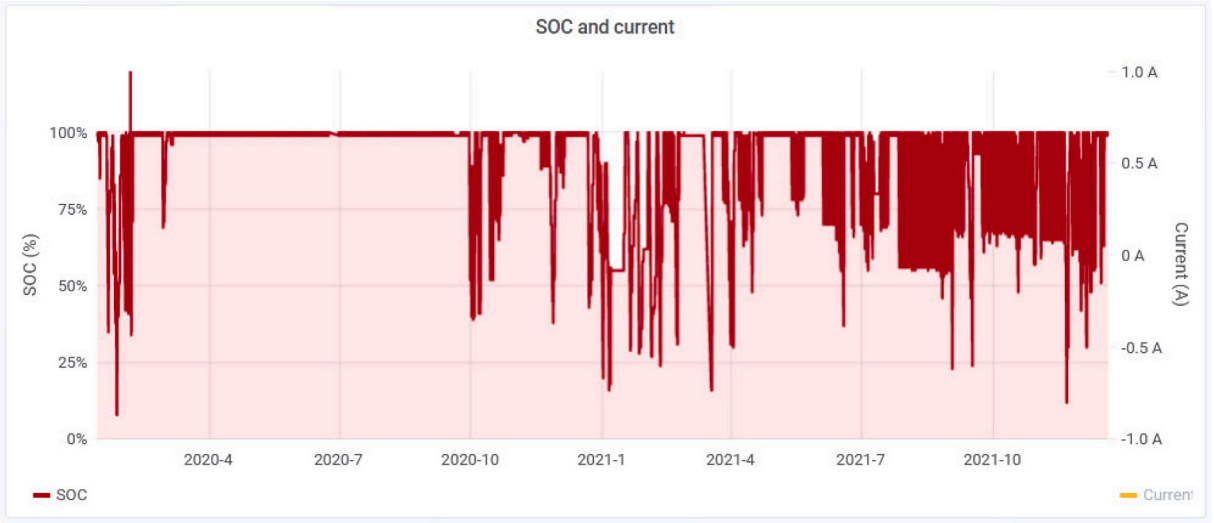

(a)

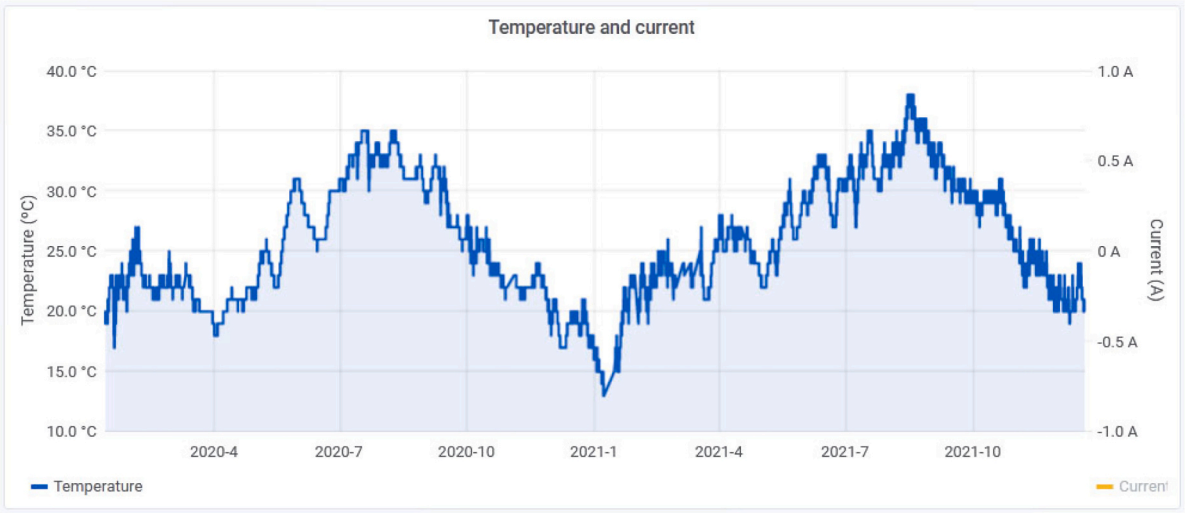

(b)

Fig. 15. Visualization of LiB data from January 2020 to December 2021: a) Temperature; b) SOC.

appears, also in green color, to indicate when the alert has finished. This way, the alert acts as a complementary of the BMU, showing the evolution of the SOC and highlighting the value under the threshold for the user to take countermeasures before a deep discharge. Even, custom-tailored alerts and thresholds can be generated for different R&D purposes like charging/discharging tests, etc.

In a similar sense, given the abovementioned importance of the LiB temperature, an alert has also been included to detect values outside the recommended range. Fortunately, such alerts have not been activated to date.

4.1.2.10. LiB discharging procedure. The proposal also serves as a tool for recording and displaying data of LiB testing under controlled laboratory conditions. An example consists on charge and discharge tests at a constant current, commonly used to check the battery operation and to obtain data for modeling purposes [7]. As a proof of concept, a discharge procedure has been carried out with a constant current of 10 A (0.1C) and starting with the LiB fully charged, illustrated in Fig. 17. The evolution of the voltage is observed in Fig. 17a; the initial value is 53.34 V and a final voltage of 51.36 V is reached. The trend of this curve presents homomorphism with the curve provided in the datasheet of the module U3A1-50P-A for a discharge current of 5 A [61] and with that reported in [7] for 20 A. On the other hand, the SOC varies in a linear manner from the initial value of 100% (at 12:11) down to 20% after 8 h 40 min (Fig. 17b).

4.2. Discussion

The developed system has been validated through experimental results over long-term period (two years) for continuous monitoring of a LiB that acts as the backbone of a microgrid with PV power to generate green hydrogen.

Online networked access to real time data of the LiB is enabled by means of IoT technology. Charging and discharging cycles can be visualized in real time or selecting the period of interest. Both developers and remote users have a large amount of customization and configuration possibilities to achieve interactive and user-friendly display of the LiB information. This feature is particularly relevant for R&D tasks [33,34]. Moreover, Grafana plug-ins are being continuously being developed and can be incorporated to the reported interface in order to

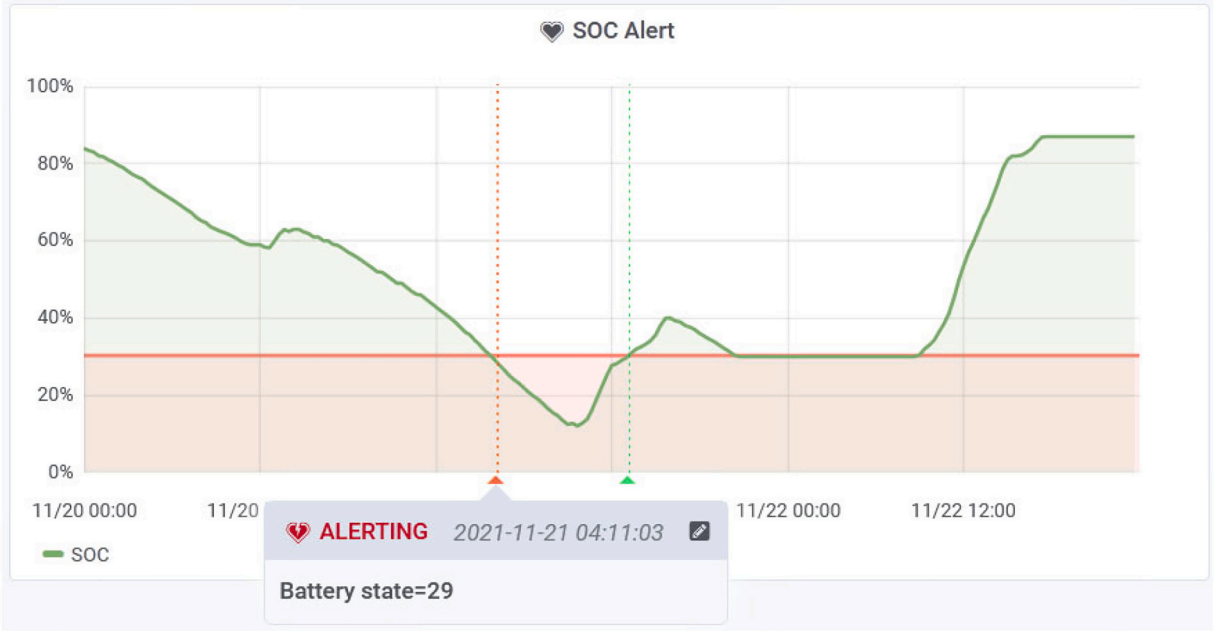

Fig. 16. Panel for SOC alert visualization.

enhance its interactivity and functionalities.

Data visualization and storage are successfully performed by the IoT server implemented in the Raspberry Pi. This avoids dependencies on external servers and provides a greater degree of freedom to the developer [14].

Safe and reliable operation of the LiB requires continuous gathering, visualization and evaluation of SOC and temperature. The monitoring system performs these tasks successfully by means of graphical and numerical displays, as well as through alerts to detect outranging of such magnitudes.

The proposal is versatile since it can be applied for continuous monitoring of the LiB under real operating conditions, as well as for data acquisition and storage during laboratory tests under controlled conditions.

The proposal is scalable and configurable to fulfil the requirements of facilities with larger LiBs. In this sense, the proposed system can be easily adapted to configurations with more BMUs simply by replicating the charts and dashboards to visualize the magnitudes of the installed modules. This capability is applicable to third-party LiBs given the wide availability of communication protocols that the Raspberry Pi and the applied software can handle.

The high cost of LiBs is considered as their main drawback [5]. In this regard, the low-cost of the developed system helps to mitigate such high costs by avoiding the high expenses of traditional solutions. It also contributes to more sustainable scientific equipment [74], to low-cost monitoring [73] and, hence, to the deployment of energy facilities around LiBs. Particularly, the involved software (mariaDB, Python and Grafana) is cost free; all packages can be directly downloaded from the Internet. About hardware, it is of low-cost nature, namely, the microcomputer Raspberry Pi can be purchased for around EUR 40. In contrast, a traditional solution involving proprietary hardware and software licenses could imply thousands of euros.

Even more, the proposal is a proof of concept of the suitability and validity of IoT and open-source technologies to gather data and monitor sophisticated and complex equipment for long-term periods. Research efforts are necessary to ensure stable operation of IoT and open-source technology when critical equipment is handled [75].

In a similar sense, the experimental microgrid constitutes an illustrative case of application of the developed system. However, it is applicable and expandable to other types of LiB-based infrastructures. In fact, the paper is expected to help in the selection of equipment and design of LiB-based facilities, since it can serve as a guide for the design of interactive and informative monitoring interfaces as well as for managing interoperability.

Indeed, the contribution to the UN Sustainable Development Goals (SDGs) are emphasized in recent research for both LiBs [76] and IoT [77].

The designed system can be applied to LiB monitoring in electric vehicles. This scenario also receives research efforts for battery management and monitoring [53,78]. Practical aspects must be taken into account, such as vibrations transmitted to the electronic boards during long-term operation, and connectivity issues, given the fact that electric vehicles can present discontinuities in wireless communication.

A limitation of the proposal which should be mentioned is related to the needed programming expertise in the design and implementation stage. This type of skills is required for advanced configurations of both hardware and software functionalities.

The acquired and accumulated data of the LiB can be used for modeling, performance analyses and prognostics. As indicated in the introductory section, a lot of research efforts are being devoted to studying the behavior of LiBs for estimating their lifetime, SOC, SOH, etc., where a large amount of data is required. For example, SOH estimation is essential for life evaluation, and health management and diagnostic of LiBs [54,55]. In a similar sense, the large amount of literature about advanced methods for SOC estimation [51–53,56,57,65,66] highlight the relevance of this magnitude for LiB operation.

5. Conclusions

This paper has presented an IoT-based monitoring system for a LiB. The LiB acts as the DC bus of a green hydrogen microgrid. The developed interface stores and illustrates the magnitudes of the battery in real time by means of time series graphs. A Raspberry Pi acts as web server and also as Modbus TCP/IP client, whereas a commercial gateway plays the role of server and provides the LiB variables. The open-source suite Grafana is applied to implement intuitive interfaces for easy interaction with the monitored process. Thanks to the IoT features, the user can access online through web navigators for continuous tracking of the LiB status and behavior.

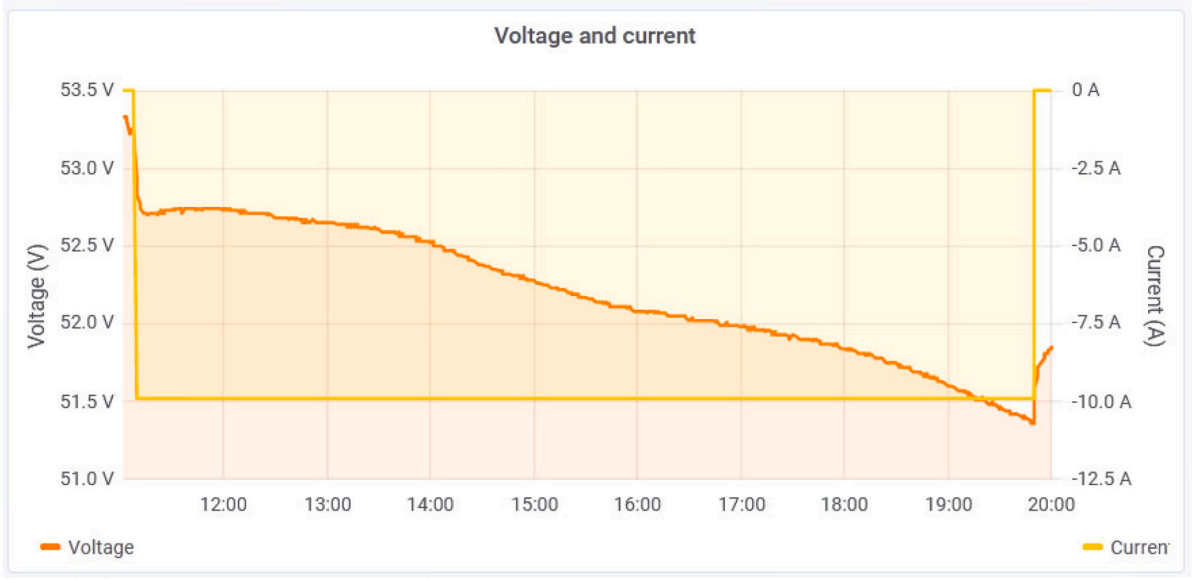

(a)

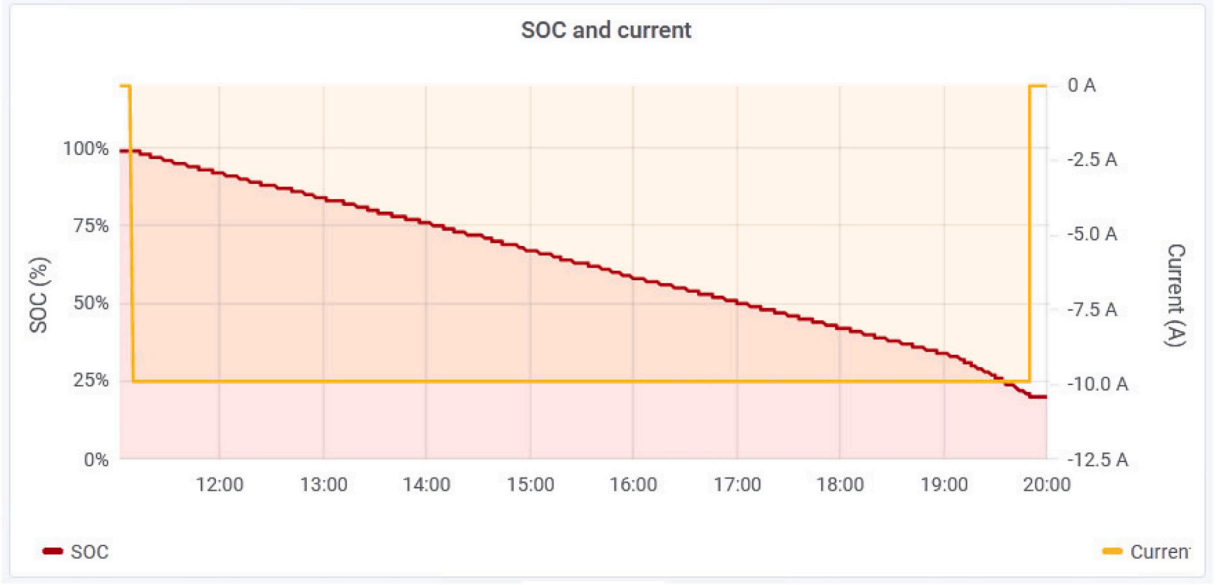

(b)

Fig. 17. Discharge procedure at constant 10 A: a) Voltage and current evolution; b) SOC and current evolution.

Experimental results have been reported in order to prove the suitability and successful operation of the developed solution. Specifically, a BYD LiB has been monitored over two years of continuous operation and its most significant magnitudes have been expounded and analyzed. In fact, voltage, current, power, temperature and SOC of the LiB have been properly monitored regarding instant values as well as trends and evolution over time.

The novelty of the development relies not only on the applied IoT technology but also in the fact that limitations identified in previous works have been overcome. Namely, this work provides long-term operation, medium-scale power/capacity LiB, alerts to track essential magnitudes, real operating conditions, as well as compatibility/interoperability handling.

The proposal is envisioned to facilitate the design and deployment of energy storage solutions through LiBs, mainly in compatibility and interoperability aspects, and implementation of monitoring systems with IoT technology.

The retrieved data are also stored for digital twining purposes, which constitute the main future research guideline. Namely, artificial intelligence methods will take advantage of such data. Statistical analyses of the results will allow for determining performance and error metrics of the LiB monitoring. Moreover, SOC and SOH estimation will also be addressed in further works.

CRediT authorship contribution statement

Isaías González: Conceptualization, Methodology, Investigation, Writing-Original Draft Preparation, Writing-Review & Editing. **Antonio José Calderón:** Conceptualization, Methodology, Validation, Investigation, Data Curation, Writing-Review & Editing, Supervision.

Francisco Javier Folgado: Investigation, Data Curation, Writing-Review & Editing.

Declaration of competing interest

The authors declare that they have no known competing financial interests or personal relationships that could have appeared to influence the work reported in this paper.

Acknowledgments

This project was co-financed by European Regional Development Funds FEDER and by the Junta de Extremadura (IB18041).

References

[1] S. Li, H. He, J. Li, Big data driven lithium-ion battery modeling method based on SDAE-ELM algorithm and data pre-processing technology, Appl. Energy 242 (2019) 1259–1273, https://doi.org/10.1016/j.apenergy.2019.03.154.
[2] R. Zhang, B. Xia, B. Li, L. Cao, Y. Lai, W. Zheng, et al., State of the art of lithium-ion battery SOC estimation for electrical vehicles, Energies. 11 (2018), https://doi.org/10.3390/en11071820.
[3] H.A. Gabbar, A.M. Othman, M.R. Abdussami, Review of battery management systems (BMS) development and industrial standards, Technologies. 9 (2021) 28, https://doi.org/10.3390/technologies9020028.
[4] A. Mashlakov, L. Lensu, A. Kaarna, V. Tikka, S. Honkapuro, Probabilistic forecasting of battery energy storage state-of-charge under primary frequency control, IEEE J. Sel. Areas Commun. 38 (2020) 96–109, https://doi.org/10.1109/JSAC.2019.2952195.
[5] R. Georgious, R. Refaat, J. Garcia, A.A. Daoud, Review on energy storage systems in microgrids, Electronics 10 (2021), https://doi.org/10.3390/electronics10172134.
[6] J.L. Torres-Moreno, A. Gimenez-Fernandez, M. Perez-Garcia, F. Rodriguez, Energy management strategy for micro-grids with PV-battery systems and electric vehicles, Energies 11 (2018), https://doi.org/10.3390/en11030522.
[7] F.J. Gómez, L.J. Yebra, A. Giménez, J.L. Torres-Moreno, Modelling of batteries for application in light electric urban vehicles, RIAI Rev. Iberoam. Autom. Inform. Ind. 16 (2019) 459–466, https://doi.org/10.4995/riai.2019.10609.
[8] I. González, A.J. Calderón, J.M. Portalo, Innovative multi-layered architecture for heterogeneous automation and monitoring systems: application case of a photovoltaic smart microgrid, Sustainability 13 (2021) 1–24, https://doi.org/10.3390/su13042234.
[9] K.S. Na, J. Lee, J.M. Kim, Y.S. Lee, J. Yi, C.Y. Won, Power conversion system operation algorithm for efficient energy management of microgrids, Electronics 10 (2021), https://doi.org/10.3390/electronics10222791.
[10] K. Santos-Pereira, J.D.F. Pereira, L.S. Veras, D.L.S. Cosme, D.Q. Oliveira, O. R. Saavedra, The requirements and constraints of storage technology in isolated microgrids: a comparative analysis of lithium-ion vs. lead-acid batteries, Energy Syst. (2021), https://doi.org/10.1007/s12667-021-00439-7.
[11] C. Vargas-Salgado, J. Aguila-Leon, C. Chiñas-Palacios, E. Hurtado-Perez, Low-cost web-based supervisory control and data acquisition system for a microgrid testbed: a case study in design and implementation for academic and research applications, Heliyon. 5 (2019), https://doi.org/10.1016/j.heliyon.2019.e02474.
[12] D. Astolfi, F. Castellani, A. Lombardi, L. Terzi, Data-driven wind turbine aging models, Electr. Power Syst. Res. 201 (2021), https://doi.org/10.1016/j.epsr.2021.107495.
[13] J. Kusznier, W. Wojtkowski, IoT solutions for maintenance and evaluation of photovoltaic systems, Energies. 14 (2021) 8567, https://doi.org/10.3390/en14248567.
[14] J.M. Portalo, I. González, A.J. Calderón, Monitoring system for tracking a pv generator in an experimental smart microgrid: an open-source solution, Sustainability 13 (2021), https://doi.org/10.3390/su13158182.
[15] P.De Arquer Fernández, M.Angel Fernández Fernández, J. Luis, C. Candás, P. Arboleya Arboleya, An IoT open source platform for photovoltaic plants supervision, Electr. Power Energy Syst. 125 (2021), 106540, https://doi.org/10.13039/501100011033.
[16] Z. Vale, H. Morais, P. Faria, C. Ramos, Distribution system operation supported by contextual energy resource management based on intelligent SCADA, Renew. Energy 52 (2013) 143–153, https://doi.org/10.1016/j.renene.2012.10.019.
[17] M. Soshinskaya, W.H.J. Crijns-Graus, J.M. Guerrero, J.C. Vasquez, Microgrids: experiences, barriers and success factors, Renew. Sust. Energ. Rev. 40 (2014) 659–672, https://doi.org/10.1016/j.rser.2014.07.198.
[18] M.A. Sanchez-Hidalgo, M.D. Cano, A survey on visual data representation for smart grids control and monitoring, Sustain. Energy Grids Netw. 16 (2018) 351–369, https://doi.org/10.1016/j.segan.2018.09.007.
[19] P. Pawar, P.K. Vittal, Design and development of advanced smart energy management system integrated with IoT framework in smart grid environment, J. Energy Storage 25 (2019), https://doi.org/10.1016/j.est.2019.100846.
[20] R.I.S. Pereira, I.M. Dupont, P.C.M. Carvalho, S.C.S. Jucá, IoT embedded linux system based on raspberry pi applied to real-time cloud monitoring of a decentralized photovoltaic plant, Meas. J. Int. Meas. Confed. 114 (2018) 286–297, https://doi.org/10.1016/j.measurement.2017.09.033.
[21] A.M. Eltamaly, M.A. Alotaibi, A.I. Alolah, M.A. Ahmed, Iot-based hybrid renewable energy system for smart campus, Sustainability 13 (2021), https://doi.org/10.3390/su13158555.
[22] N. Mohammed, A.M. Saif, Programmable logic controller based lithium-ion battery management system for accurate state of charge estimation, Comput. Electr. Eng. 93 (2021), https://doi.org/10.1016/j.compeleceng.2021.107306.
[23] J.K. Thomas, H.R. Crasta, K. Kausthubha, C. Gowda, A. Rao, Battery monitoring system using machine learning, J. Energy Storage. 40 (2021), https://doi.org/10.1016/j.est.2021.102741.
[24] G.R. Sylvestrin, H.R. Scherer, O.H. Ando, Hardware and software development of an open source battery management system, IEEE Lat. Am. Trans. 19 (2021) 1153–1163.
[25] P. Lezynski, P. Szczesniak, B. Waskowicz, R. Smolenski, W. Drozdz, Design and implementation of a fully controllable cyber-physical system for testing energy storage systems, IEEE Access. 7 (2019) 47259–47272, https://doi.org/10.1109/ACCESS.2019.2907612.
[26] E. Vergori, F. Mocera, A. Somà, Battery modelling and simulation using a programmable testing equipment, Computers. 7 (2018), https://doi.org/10.3390/computers7020020.
[27] L. Guo, J. Li, Z. Fu, Lithium-ion battery SOC estimation and hardware-in-the-loop simulation based on EKF, Energy Procedia 158 (2019) 2599–2604, https://doi.org/10.1016/j.egypro.2019.02.009. Elsevier Ltd.
[28] H. Samanta, A. Bhattacharjee, M. Pramanik, A. Das, K. Das Bhattacharya, H. Saha, Internet of things based smart energy management in a vanadium redox flow battery storage integrated bio-solar microgrid, J. Energy Storage 32 (2020), https://doi.org/10.1016/j.est.2020.101967.
[29] N. Hosseinzadeh, A. Al Maashri, N. Tarhuni, A. Elhaffar, A. Al-Hinai, A real-time monitoring platform for distributed energy resources in a microgrid—pilot study in Oman, Electronics 10 (2021), https://doi.org/10.3390/electronics10151803.
[30] S. Li, H. He, C. Su, P. Zhao, Data driven battery modeling and management method with aging phenomenon considered, Appl. Energy 275 (2020), https://doi.org/10.1016/j.apenergy.2020.115340.
[31] R. Lu, J. Lu, P. Liu, M. He, J. Liu, Design of the vrla battery real-time monitoring system based on wireless communication, Sensors 20 (2020) 1–17, https://doi.org/10.3390/s20154350.
[32] A. Trovò, Battery management system for industrial-scale vanadium redox flow batteries: features and operation, J. Power Sources 465 (2020), https://doi.org/10.1016/j.jpowsour.2020.228229.
[33] I. González, A.J. Calderón, J.M. Andújar, Novel remote monitoring platform for RES-hydrogen based smart microgrid, Energy Convers. Manag. 148 (2017) 489–505, https://doi.org/10.1016/j.enconman.2017.06.031.
[34] A.A. Smadi, B.T. Ajao, B.K. Johnson, H. Lei, Y. Chakhchoukh, Q.Abu Al-Haija, A comprehensive survey on cyber-physical smart grid testbed architectures: requirements and challenges, Electronics 10 (2021) 1043, https://doi.org/10.3390/electronics10091043.
[35] F.J. Gimeno-Sales, S. Orts-Grau, A. Escribá-Aparisi, P. González-Altozano, I. Balbastre-Peralta, C.I. Martínez-Márquez, et al., Pv monitoring system for a water pumping scheme with a lithium-ion battery using free open-source software and iot technologies, Sustainability 12 (2020) 1–28, https://doi.org/10.3390/su122410651.
[36] S. Orts-Grau, P. Gonzalez-Altozano, F.J. Gimeno-Sales, I. Balbastre-Peralta, C.I. M. Marquez, M. Gasque, et al., Photovoltaic water pumping: comparison between direct and lithium battery solutions, IEEE Access. 9 (2021) 101147–101163, https://doi.org/10.1109/ACCESS.2021.3097246.
[37] A.K.L. Ghanima, B. Nadir, Efficiency evaluation of experimental (photovoltaic -wind) hybrid system with the effect of maximum power point tracking charge controller to the production of valve regulated lead-acid batteries in Constantine-Algeria, J. Energy Storage. 41 (2021), https://doi.org/10.1016/j.est.2021.102856.
[38] C. Zou, C. Manzie, D. Nešić, A.G. Kallapur, Multi-time-scale observer design for state-of-charge and state-of-health of a lithium-ion battery, J. Power Sources 335 (2016) 121–130, https://doi.org/10.1016/j.jpowsour.2016.10.040.
[39] L. Komsiyska, T. Buchberger, S. Diehl, M. Ehrensberger, C. Hanzl, C. Hartmann, et al., Critical review of intelligent battery systems: challenges, implementation, and potential for electric vehicles, Energies. 14 (2021), https://doi.org/10.3390/en14185989.
[40] A. Samanta, S.S. Williamson, A comprehensive review of lithium-ion cell temperature estimation techniques applicable to health-conscious fast charging and smart battery management systems, Energies. 14 (2021), https://doi.org/10.3390/en14185960.
[41] N. Jamil, Q.S. Qassim, F.A. Bohani, M. Mansor, V.K. Ramachandaramurthy, Cybersecurity of microgrid: state-of-the-art review and possible directions of future research, Appl. Sci. 11 (2021) 9812, https://doi.org/10.3390/app11219812.
[42] A.S. Ali, C. Coté, M. Heidarinejad, B. Stephens, Elemental: an open-source wireless hardware and software platform for building energy and indoor environmental monitoring and control, Sensors 19 (2019), https://doi.org/10.3390/s19184017.
[43] M.D. Mudaliar, N. Sivakumar, IoT based real time energy monitoring system using raspberry Pi, Internet Things 12 (2020), https://doi.org/10.1016/j.iot.2020.100292.
[44] C. Liu, Z. Su, X. Xu, Y. Lu, Service-oriented industrial internet of things gateway for cloud manufacturing, Robot. Comput. Integr. Manuf. 73 (2022), https://doi.org/10.1016/j.rcim.2021.102217.
[45] Y. Miao, P. Hynan, A. Von Jouanne, A. Yokochi, Current li-ion battery technologies in electric vehicles and opportunities for advancements, Energies. 12 (2019), https://doi.org/10.3390/en12061074.

[46] Y. Chen, X. Yang, D. Luo, R. Wen, Remaining available energy prediction for lithium-ion batteries considering electrothermal effect and energy conversion efficiency, J. Energy Storage. 40 (2021), https://doi.org/10.1016/j.est.2021.102728.
[47] S. Wang, S. Jin, D. Deng, C. Fernandez, in: A Critical Review of Online Battery Remaining Useful Lifetime Prediction Methods 7, 2021, pp. 1–19, https://doi.org/10.3389/fmech.2021.719718.
[48] S. Wang, S. Jin, D. Bai, Y. Fan, H. Shi, C. Fernandez, A critical review of improved deep learning methods for the remaining useful life prediction of lithium-ion batteries, Energy Rep. 7 (2021) 5562–5574, https://doi.org/10.1016/j.egyr.2021.08.182.
[49] P. Wang, L. Yang, H. Wang, D.M. Tartakovsky, S. Onori, Temperature estimation from current and voltage measurements in lithium-ion battery systems, J. Energy Storage. 34 (2021), https://doi.org/10.1016/j.est.2020.102133.
[50] J. Wu, X. Liu, J. Meng, M. Lin, Cloud-to-edge based state of health estimation method for Lithium-ion battery in distributed energy storage system, J. Energy Storage. 41 (2021), https://doi.org/10.1016/j.est.2021.102974.
[51] Z. Wei, S. Meng, B. Xiong, D. Ji, K. Jet, Enhanced online model identification and state of charge estimation for lithium-ion battery with a FBCRLS based observer, Appl. Energy 181 (2016) 332–341, https://doi.org/10.1016/j.apenergy.2016.08.103.
[52] Z. Wei, Online Model Identification and State-of-Charge Estimate for Lithium-Ion Battery With a Recursive Total Least Squares-Based Observer, 2018.
[53] Z. Wei, J. Hu, Y. Li, H. He, W. Li, D.U. Sauer, Hierarchical soft measurement of load current and state of charge for future smart lithium-ion batteries, Appl. Energy 307 (2022), 118246, https://doi.org/10.1016/j.apenergy.2021.118246.
[54] Z. Wei, H. Ruan, Y. Li, J. Li, C. Zhang, H. He, in: Multistage State of Health Estimation of Lithium-Ion Battery With High Tolerance to Heavily 37, 2022, pp. 7432–7442.
[55] H. Ruan, H. He, S. Member, Z. Wei, S. Member, State of Health Estimation of Lithium-ion Battery Based on Constant-Voltage Charging Reconstruction 6777, 2021, https://doi.org/10.1109/JESTPE.2021.3098836.
[56] S. Wang, C. Fernandez, C. Yu, Y. Fan, W. Cao, D. Stroe, A novel charged state prediction method of the lithium ion battery packs based on the composite equivalent modeling and improved splice Kalman filtering algorithm, J. Power Sources 471 (2020), 228450, https://doi.org/10.1016/j.jpowsour.2020.228450.
[57] S. Wang, in: A Novel Safety Assurance Method Based on the Compound Equivalent Modeling and Iterate Reduce Particle-Adaptive Kalman Filtering for the Unmanned Aerial Vehicle Lithium Ion Batteries, 2020, pp. 1484–1500, https://doi.org/10.1002/ese3.606.
[58] X. Sui, M. Świerczyński, R. Teodorescu, D.I. Stroe, The degradation behavior of lifepo4/c batteries during long-term calendar aging, Energies. 14 (2021), https://doi.org/10.3390/en14061732.
[59] M.K. Tran, A. Dacosta, A. Mevawalla, S. Panchal, M. Fowler, Comparative study of equivalent circuit models performance in four common lithium-ion batteries: LFP, NMC, LMONCA, Batteries 7 (2021), https://doi.org/10.3390/batteries7030051.
[60] Y.D. Su, Y. Preger, H. Burroughs, C. Sun, P.R. Ohodnicki, Fiber optic sensing technologies for battery management systems and energy storage applications, Sensors 21 (2021) 1–36, https://doi.org/10.3390/s21041397.
[61] BYD U3A1-50P-A Module Specifications: https://sg.byd.com/wp-content/uploads/2018/05/3U-Spec._20180315.pdf (accessed on December 2021) n.d.
[62] F.J. Vivas Fernández, F.S. Manzano, J.M.A. Márquez, A.J. Calderón Godoy, Extended model predictive controller to develop energy management systems in renewable source-based smart microgrids with hydrogen as backup. Theoretical foundation and case study, Sustainability 12 (2020) 1–28, https://doi.org/10.3390/su12218969.
[63] M. Kermani, B. Adelmanesh, E. Shirdare, C.A. Sima, D.L. Carnì, L. Martirano, Intelligent energy management based on SCADA system in a real microgrid for smart building applications, Renew. Energy 171 (2021) 1115–1127, https://doi.org/10.1016/j.renene.2021.03.008.
[64] X. Ma, D. Qiu, Q. Tao, D. Zhu, State of charge estimation of a lithium ion battery based on adaptive kalman filter method for an equivalent circuit model, Appl. Sci. 9 (2019), https://doi.org/10.3390/APP9132765.
[65] W. Cao, S.L. Wang, C. Fernandez, C.Y. Zou, C.M. Yu, X.X. Li, A novel adaptive state of charge estimation method of full life cycling lithium-ion batteries based on the multiple parameter optimization, Energy Sci. Eng. 7 (2019) 1544–1556, https://doi.org/10.1002/ese3.362.
[66] S.L. Wang, C. Fernandez, W. Cao, C.Y. Zou, C.M. Yu, X.X. Li, An adaptive working state iterative calculation method of the power battery by using the improved Kalman filtering algorithm and considering the relaxation effect, J. Power Sources 428 (2019) 67–75, https://doi.org/10.1016/j.jpowsour.2019.04.089.
[67] X. Lai, D. Qiao, Y. Zheng, L. Zhou, A fuzzy state-of-charge estimation algorithm combining ampere-hour and an extended Kalman filter for li-ion batteries based on multi-model global identification, Appl. Sci. 8 (2018), https://doi.org/10.3390/app8112028.
[68] A. Bonfitto, S. Feraco, A. Tonoli, N. Amati, F. Monti, Estimation accuracy and computational cost analysis of artificial neural networks for state of charge estimation in lithium batteries, Batteries. 5 (2019), https://doi.org/10.3390/batteries5020047.
[69] J. Kim, J. Kowal, K.P. Birke, A Method for Monitoring State-of-Charge of Lithium-Ion Cells Using Multi-Sine Signal Excitation, 2021, https://doi.org/10.3390/batteries.
[70] I. González, A.J. Calderón, A.J. Barragán, J.M. Andújar, Integration of sensors, controllers and instruments using a novel OPC architecture, Sensors 17 (2017), https://doi.org/10.3390/s17071512.
[71] M. Wollschlaeger, T. Sauter, J. Jasperneite, The future of industrial communication: automation networks in the era of the internet of things and industry 4.0, IEEE Ind. Electron. Mag. 11 (2017) 17–27, https://doi.org/10.1109/MIE.2017.2649104.
[72] S. Jaloudi, Communication protocols of an industrial internet of things environment: a comparative study, Future Internet. 11 (2019), https://doi.org/10.3390/fi11030066.
[73] G. Hawkridge, A. Mukherjee, D. McFarlane, Y. Tlegenov, A.K. Parlikad, N. J. Reyner, et al., Monitoring on a shoestring: low cost solutions for digital manufacturing, Annu. Rev. Control. 51 (2021) 374–391, https://doi.org/10.1016/j.arcontrol.2021.04.007.
[74] J.M. Pearce, Economic savings for scientific free and open source technology: a review, HardwareX. 8 (2020), https://doi.org/10.1016/j.ohx.2020.e00139.
[75] I. González, A.J. Calderón, Integration of open source hardware arduino platform in automation systems applied to smart grids/Micro-grids, Sustain. Energy Technol. Assessments. 36 (2019), https://doi.org/10.1016/j.seta.2019.100557.
[76] M.A. Hannan, A.Q. Al-Shetwi, R.A. Begum, P. Jern Ker, S.A. Rahman, M. Mansor, et al., Impact assessment of battery energy storage systems towards achieving sustainable development goals, J. Energy Storage. 42 (2021), https://doi.org/10.1016/j.est.2021.103040.
[77] M.E. Mondejar, R. Avtar, H.L.B. Diaz, R.K. Dubey, J. Esteban, A. Gómez-Morales, et al., Digitalization to achieve sustainable development goals: steps towards a smart green planet, Sci. Total Environ. 794 (2021), https://doi.org/10.1016/j.scitotenv.2021.148539.
[78] S. Li, P. Zhao, Big data driven vehicle battery management method : a novel cyber-physical system perspective, J. Energy Storage 33 (2021), 102064, https://doi.org/10.1016/j.est.2020.102064.